ELSEVIER

Physica C 294 (1998) 161–168

PHYSICA C

Texture development in $Bi_2Sr_2CaCu_2O_y$ current leads

T.G. Holesinger *, J.O. Willis, M.C. Martinez, J.Y. Coulter

Superconductivity Technology Center, Los Alamos National Laboratory, Los Alamos, NM 87545, USA

Received 25 September 1997; accepted 9 October 1997

Abstract

Isothermal melt processing has been used to partially texture bulk samples of $Bi_2Sr_2CaCu_2O_y$ (Bi-2212). Anisotropic growth of Bi-2212 occurs from the partial melt in the presence of an oxygen gradient. The orientational preference is for the *c*-axis of the Bi-2212 grains to align perpendicular to the oxygen gradient. However, the one-dimensional nature of the oxygen gradient does not result in uniaxial texture. Incorporation of a set of silver plates aligned parallel to the oxygen gradient was found to provide the second texturing mechanism needed to improve grain-to-grain alignment and start the development of uniaxial texture within bulk Bi-2212 bars. Texture within the bars was investigated by anisotropy measurements of the critical current in applied magnetic fields and compared to previously published results on Bi-2212 films. At liquid nitrogen temperatures, the presence of partial texture in the bulk Bi-2212 bars was found to increase the performance in applied fields by a factor of two relative to the untextured current leads. However, comparison of the bulk-textured bar to the Bi-2212 film revealed that the bar has a significantly larger spread in grain orientations than does the 50 μm thick film. © 1998 Elsevier Science B.V.

Keywords: Superconductor; Bi-2212; Isothermal; Melt processing

1. Introduction

The Bi-based high-temperature superconductors, $Bi_2Sr_2Ca_2Cu_3O_y$ (Bi-2223) and $Bi_2Sr_2CaCu_2O_y$ (Bi-2212), are potential candidates for use in current lead applications. Several groups have demonstrated Bi-based current leads in a variety of forms such as Ag–Au alloy-sheathed Bi-2223 tapes [1], melt-cast Bi-2212 tubes [2], sinter-forged Bi-2223 bars [3], directional growth of near single-crystal Bi-2212 fibers [4,5] and composite reaction-textured Bi-2212 bars [6]. Recently, it has been shown that highly textured $Bi_2Sr_2CaCu_2O_y$ (Bi-2212) current leads could be grown by isothermal melt processing (IMP) [7]. Isothermal melt processing is an attractive process for melt processing Bi-2212 because of the inherently lower processing temperatures required and the high critical current densities obtained in practical conductors [7–9]. During the oxidation step of IMP, an oxygen gradient is step up within the sample. Because of the anisotropy in the growth characteristics of Bi-2212, the *a*–*b*-planes preferentially grow along the direction of the oxygen gradient as the superconducting phase solidifies from the partial melt [7]. Unfortunately, the oxygen gradient provides only one degree of texture which does not produce good grain-to-grain or colony-to-colony alignment. In this paper, it is shown that uniaxial

* Corresponding author. Fax: +1 505 665 3164.

PII S0921-4534(97)01780-2

texture can be at least partially developed in bulk Bi-2212 bars during the oxidation step of IMP when combined with a second texturing mechanism. For this work, the second texturing mechanism consisted of a set of parallel silver plates spaced 2 mm apart, running the length of the current lead, and aligned parallel to the oxygen gradient.

2. Experimental

Bulk Bi-2212 current leads were produced from commercial powder (Seattle Specialty Ceramics) of composition $Bi_2Sr_{2.15}Ca_{0.85}Cu_2O_y$. This composition was chosen because it is the composition of the resulting Bi-2212 phase in isothermally melt processed samples [7]. To this powder, 1.0 wt.% Al_2O_3 was added for grain refinement of phases in the partial melt [10]. The powder was then calcined in 20%O_2/Ar for 15 h at 800°C, 820°C, and 840°C. All gases were scrubbed with commercial molecular sieves to lower the carbon and water contents. The powders were then processed by splat-quenching from 1125°C to form glassy precursors [11]. Splat-quenching produces an oxygen-deficient, amorphous precursor in which all elements, including aluminum, are thoroughly mixed at the atomic level. The crucible used during the splat-quench process was platinum. The current leads were isothermally melt processed at 840°C using oxygen for the oxidizing atmosphere. Precursor powders were loaded into silver boats of approximate dimensions 10 cm × 1 cm × 0.5 cm. For some of the current leads, 4 or 5 silver strips (10 cm × 1 cm × 0.025 cm) were inserted lengthwise into the silver boat prior to filling with powder. The spacing between strips was approximately 2 mm. During the first stage of processing, the powder was melted under vacuum for 1 h at 840°C. At the end of one hour, the furnace was backfilled with oxygen to solidify the Bi-2212 phase. The samples were held at the temperature of 840°C for an additional 99 h after which they were cooled at 3°C/min to room temperature.

Microstructure and phase identification were performed by scanning electron microscopy (SEM) with energy dispersive spectroscopy (EDS). Additional phase identification was by X-ray diffraction (XRD). Transition temperatures were measured by SQUID

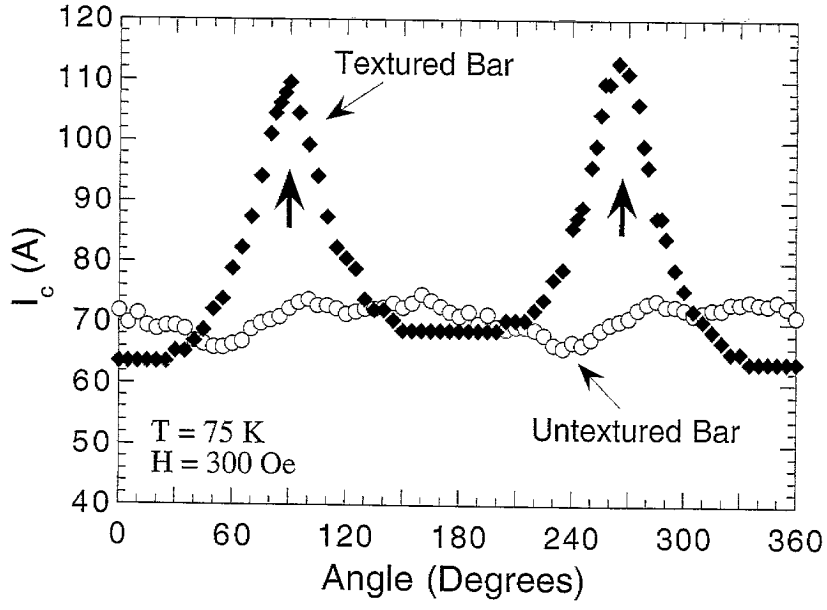

Fig. 1. Anisotropy measurements of the critical currents in textured and untextured Bi-2212 bars at 75 K in an applied field of 300 Oe.

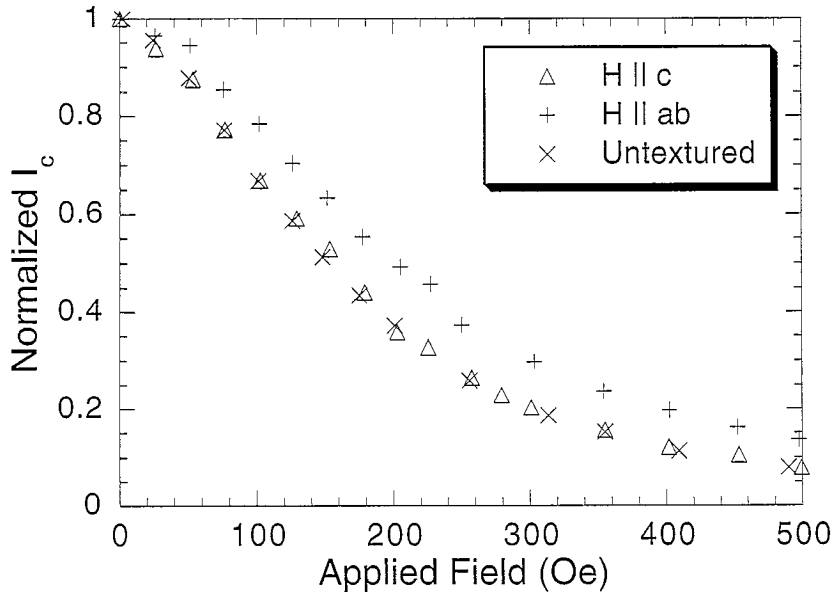

Fig. 2. Normalized critical currents as a function of applied field at 75 K for both the textured and untextured current leads.

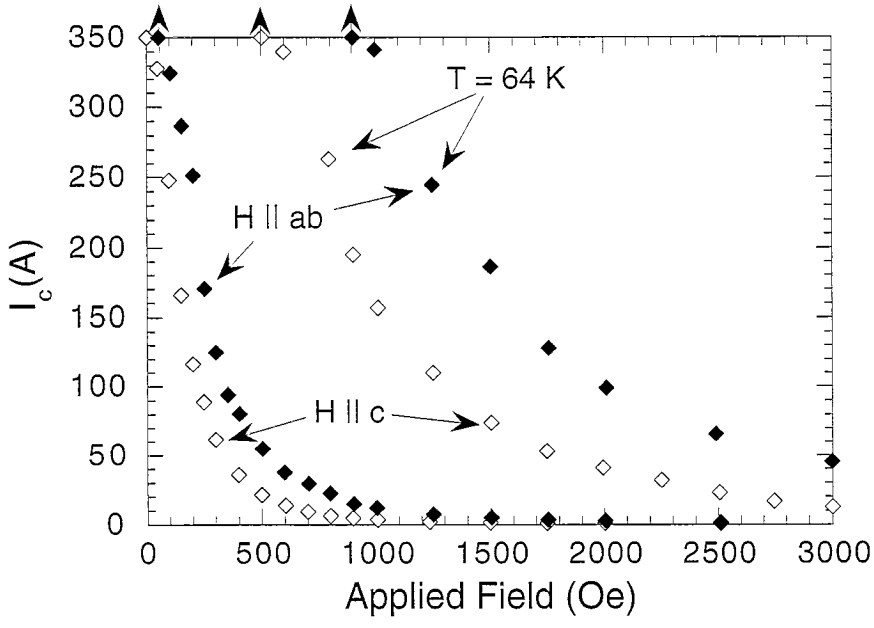

Fig. 3. Critical currents for a textured Bi-2212 bar in applied fields at 75 and 64 K (pumped liquid nitrogen).

magnetization measurements. Critical currents (I_c) and current densities (J_c) in self- and applied fields were determined from transport measurements at 75 and 64 K. Angular dependence measurements of the critical current in applied fields were used to determine the degree of orientation of the grains in the bulk Bi-2212 bars. These results were then compared to previous work on Bi-2212 thick films produced by Legendre et al. [12].

3. Results

Shown in Fig. 1 are the anisotropy measurements at 75 K of the current leads isothermally melt processed with and without the silver inserts. For the untextured current lead, the self-field I_c was 346 A at 75 K. When combined with the cross-sectional area measurement, the I_c value corresponded to a critical current density of 465 A/cm^2. No anisotropy in the transport properties was found in the sample grown without the inserts. Hence, there was no superconducting path through the bar that was uniaxially textured. The current lead processed with the silver inserts had a self-field I_c value of 340 A at 75 K. Correlation of I_c with the cross-sectional area revealed a J_c value of 570 A/cm^2. For the latter sample, anisotropy measurements showed an enhancement of I_c when H was parallel to the silver inserts. The interpretation of this result is that uniaxial texture had developed within at least a connected portion of the bulk bar. Within the portion of the bar that contained the textured material, the a–b-planes of the Bi-2212 superconductor had aligned parallel to the oxygen gradient and the silver inserts.

Fig. 2 contains plots of the normalized critical current versus applied field for both the textured and untextured leads discussed above. A greater retention in I_c by a factor of approximately two is observed in applied fields for the textured current lead. For the orientation in which the applied field is perpendicular to the faces of the silver inserts, the field dependence was found to be nearly identical to that of the untextured current lead.

The differences in retained critical currents as function of applied field for the partially textured current lead become more pronounced at lower temperatures. Fig. 3 contains the plots of I_c versus H at 75 K and 64 K (pumped liquid nitrogen) for a second textured lead. Again, the spacing between the silver inserts was 2 mm and the nominal increase in I_c in applied fields was approximately two. Note that this sample carried slightly in excess of 350 A at 75 K, the limit of the power supply. Nonetheless, Fig. 3 shows that the absolute differences in I_c as a function of field strength and direction increase as the temperature is decreased. At 64 K, the lead was found to carry in excess of 350 A at 500 Oe for $H \| c$ while it carried in excess of 350 A at 900 Oe for $H \| ab$.

Fig. 4(a),(b) contain backscattered electron micrographs of the untextured lead in both cross-section and plane-view, respectively. The microstructure of the untextured bar is made up of large Bi-2212 colonies that show a small amount of alignment

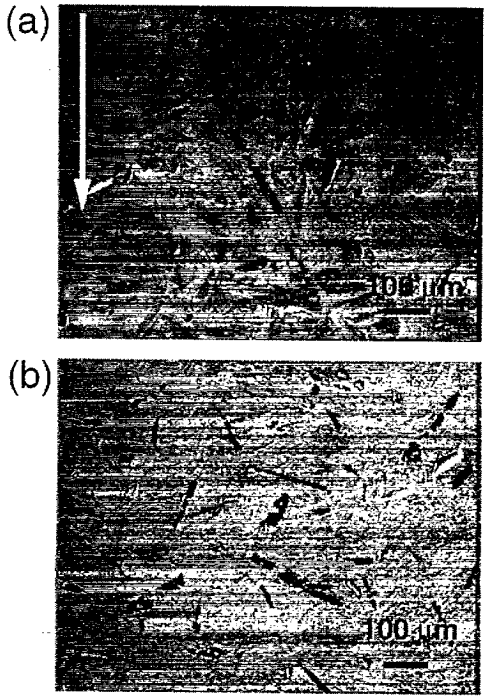

Fig. 4. Backscattered electron micrographs of the untextured bar taken in (a) cross-section looking perpendicular to the growth direction (arrow) and (b) plane-view looking down the growth direction. The large, black needles were identified as the 14:24 AEC.

relative to the growth direction in the cross-sectional micrograph. When examined in plane view, little or no alignment between individual colonies is observed. This microstructure is consistent with the anisotropy measurements presented in Figs. 1 and 2. In terms of the secondary phase assemblage, the phases identified in this sample were $Sr_{14-x}Ca_xCu_{24}O_y$ (14:24 AEC), $Bi_2Sr_{2-x}Ca_xCuO_y$ (Bi-2201), $Sr_{2-x}Ca_xAlO_y$ (2:1 AEA), and $Bi_2Sr_{4-x}Ca_xAl_3O_y$ (243 AEA). The latter two aluminates result from the additions of alumina in the starting material for grain refinement of phases in the partial melt [10].

Fig. 5(a),(b) contain secondary electron micrographs of a textured lead in both cross-section and plane-view, respectively. In the cross-sectional view, the Bi-2212 grains or colonies are in relatively good alignment over the distance of 2 mm between the silver inserts. In plane view, Fig. 5(b), large Bi-2212 colonies are again oriented along the silver insert although some colonies can be found with orientations perpendicular to the silver insert. Hence, the bulk material is not completely textured as will be evident below when the comparison is made to Bi-2212 thick films. Nonetheless, it is clear from the micrographs of Fig. 5 and the anisotropy measurements of Figs. 1 and 2 that a connected portion of Bi-2212 colonies have aligned themselves parallel to the silver inserts, hence to each other, and formed a uniaxially textured microstructure with the character-

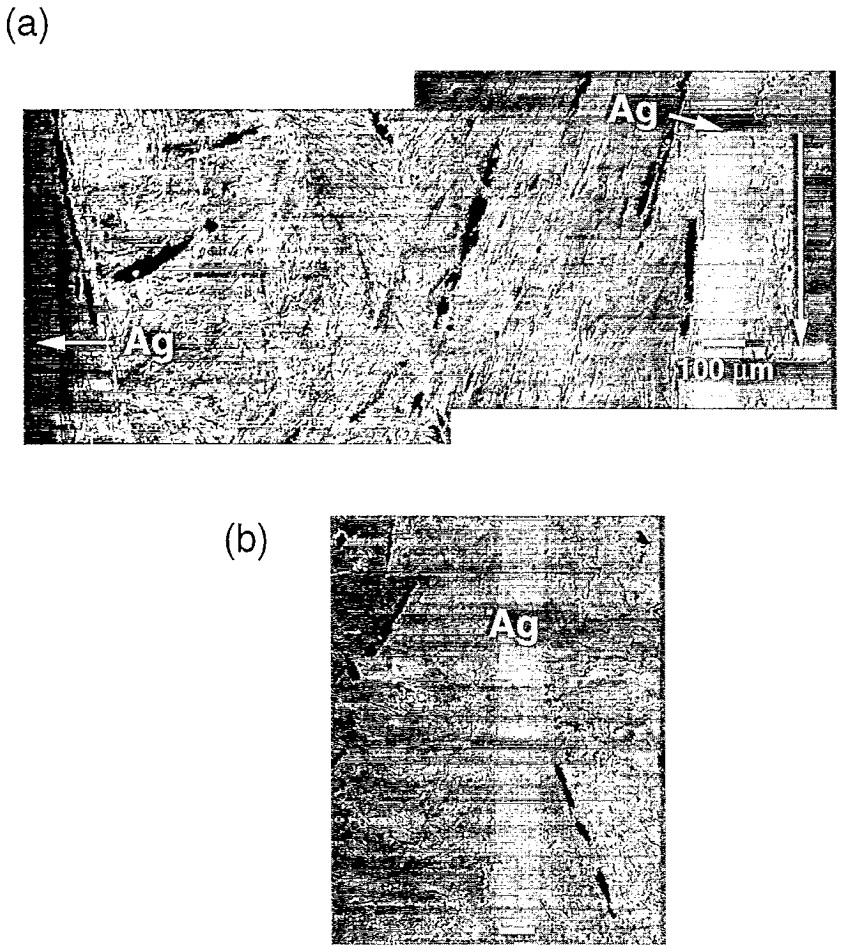

Fig. 5. Backscattered electron micrographs of the textured bar taken in (a) cross-section looking perpendicular to the growth direction (arrow) and (b) plane-view looking down the growth direction. The large, black needles were identified as the 14:24 AEC.

istic anisotropy in transport properties in applied magnetic fields. The secondary phase assemblage of the Bi-2212 bar in Fig. 5 consists of 14:24 AEC, Bi-2201, 2:1 AEA, and 243 AEA. Overall, the phase assemblages in both the textured and untextured bars were identical and T_c measurements revealed identical T_c values of 94 K.

Several methods were employed to determine the degree of orientation of the Bi-2212 grains in the bars. To begin, the I_c values for the bar were determined at voltage criteria of 1 and 0.2 μV/cm (1 μV along the 5 cm gauge length in the measurement). In addition, the current–voltage curves were fitted over the range 0 to 20 μV to the model described by Gurevitch et al. [13]: $I = I_c + I_1 \ln(V/V_c) + V/R$ and were evaluated with $V_c = 1$ μV. In this expression, R can be related to the parallel resistance of the Ag sheets embedded in the bars and had values in the range 0.3 to 0.6 μΩ for $H \| c$ and $H > 50$ Oe; the value at 0 Oe was much larger at 1.23 μΩ, however the fitting range for the voltage was restricted to 0 to 10 μV because of the large I_c and the power supply maximum current limit. The values for I_c are in very good agreement with those derived from the direct analysis of the I/V data using the 0.2 μV/cm ($V = 1$ μV) criterion, as expected. It was found that the data for I_c (0.2 μV/cm) showed slightly higher anisotropy than that for I_c (1 μV/cm). This is because at the higher electric field criterion and high fields, where the I_c is small, relatively more current flows through the Ag plates, thus reducing the anisotropy.

The I_c vs. magnetic field and I_c vs. angle data were then analyzed to determine the degree of orientation of the grains in the bars. The analytical models are all based on the extreme electronic anisotropy of Bi-2212 at temperatures above about 20–30 K that yields a critical current density that depends only upon the c-axis component of an applied field. If we define as ϕ the angle that the magnetic field makes with respect to the c-axis of a single crystal of Bi-2212, then $J_c(B(\phi)) \approx J_{c(\phi=0)}(B\cos\phi)$, where $J_{c(\phi=0)}$ is J_c for the field along the c-axis. This model has been applied to the analysis of the degree of orientation of the Bi-2212 grains in thin films by Legendre et al. [12] and of the texture of Bi-2223/Ag sheathed tapes by Hu et al. [14] and by Willis et al. [15]. The model works quite well when the spread in

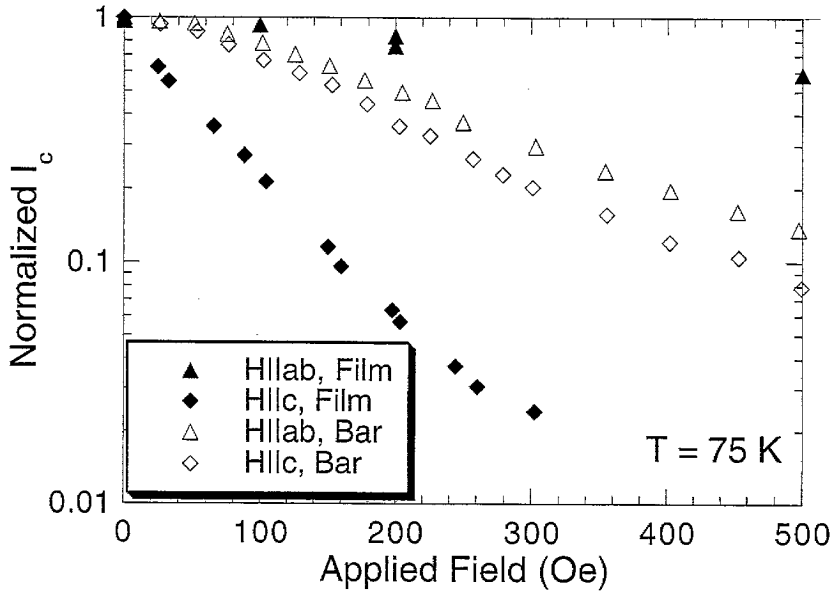

Fig. 6. Plot of the normalized critical currents as a function of applied field at 75 K for the textured current lead and the thick film from Legendre et al. [12].

Table 1
Determination of the grain orientation spread θ for the Bi-2212 samples by three methods

Method of obtaining θ	Film [a] Film [a]	Textured bar $E = 1$ μV/cm	Textured bar $E = 0.2$ μV/cm	Untextured bar
Deviation from $H\cos\phi$ (°)	3.5			–
Scaling of $J_c(90°)$ by $H\cos\phi$ (°)	3.0	38	35	90
$\arcsin(H_2/H_1)$ (°)	3.3	50	44	90

[a] Raw data from Legendre et al. [12].

the c-axis orientation of the grains is relatively small, i.e., less than about 30°. The value of $90° - \phi$ at which the $B\cos\phi$ dependence breaks down is a good measure of the average spread in grain orientations θ. $J_c(\phi = 90°)$ can also be scaled onto the $J_c(\phi = 0°)$ data by plotting the former vs. $H\cos\phi$ and the latter vs. H or, more accurately for larger orientation spreads, $H\sin\phi$. When these two curves coincide, $90° - \phi$ is another measure of the spread in orientation θ. Fig. 6 shows the normalized I_c data for a Bi-2212 film of Legendre et al. and data for the textured current lead. The film had θ values of 3.5° and 3° by the two methods discussed above; this is a very highly aligned Bi-2212 sample. In contrast, the data for the textured bar could not be fit using the first method. This is believed to be due to the relatively low degree of texture for the bar, or in other words, to a relatively large θ value. The second method yielded θ values of 38° and 35° for I_c criteria of 1 and 0.2 μV/cm, respectively. Hu et al. proposed another method to determine θ based on the fact that at a given magnetic field value H_1, J_c varies from a minimum of $J_c(H_1, \phi = 0°)$ to a maximum of $J_c(H_1, \phi = 90°)$, and that there is another point H_2 ($H_2 < H_1$) such that $J_c(H_2, \phi = 0°) = J_c(H_1, \phi = 90°)$. The grain orientation spread θ can be deduced as $\theta = \arcsin(H_2/H_1)$. Applying this model to the Bi-2212 film sample at 7 points in the range 600 Oe $< H_1 <$ 4000 Oe yielded θ values from 3° to 3.6° in good agreement with the earlier methods. The textured bar yielded θ values of about 50° and 44° for I_c criteria of 1 and 0.2 μV/cm, respectively. These results are summarized in Table 1 comparing the different methods for estimating θ and the values that would be obtained for the untextured bar.

Although the values for θ vary quantitatively depending on the method used to analyze the I_c data for the textured bar, the trends are qualitatively similar. To summarize the results, the textured bar shows a significantly smaller value of θ than does the untextured bar. The result is a current lead that has similar J_c field dependence to an untextured lead for the field parallel to the broad face of the lead, and clearly enhanced performance for the magnetic field perpendicular (parallel to the inserts) to the flat face of the current lead.

4. Discussion

Oxygen gradients are typically encountered when melt processing Bi-2212 regardless of whether the technique employed is conventional or isothermal melt processing. In "two-dimensional" conductors such as tapes or thick films, the sheath material, substrate, or even free surface is typically the dominant texturing force [16]. However, in the case of bulk or "three-dimensional" shapes, oxygen gradients become important texturing mechanisms. Note that the oxygen gradient is established during the early stages of the oxidation process of IMP and is not present in the fully processed material. It is used in the present context as a reference frame to describe the microstructural features and their origins in the bulk Bi-2212 bars.

The observed texture development in bulk bars described above cannot be ascribed to silver inserts alone. As shown in Fig. 5(a), good alignment of the Bi-2212 grains can extend up to 1 mm from silver inserts. During thick film processing, it is typically found that the maximum thickness that can be textured is 50 μm or less. Hence the beneficial effects of the silver inserts and oxygen gradient are additive in the development of texture during the processing of the bulk bars. Clearly, the same level of texture

that was observed in the thick films has not been achieved yet in the bulk bars. The initial spacing of 2 mm between silver sheets was only used as a starting point as optimal spacing and processing conditions are yet to be determined. However, the factor of two improvement in field performance is important when considering applications such as current leads. Note that the partial development of uniaxial texture was achieved in the bulk Bi-2212 bars with only a simple furnace heat treatment. No mechanical deformation steps or special crystal growth techniques were used.

5. Summary

It was shown that the oxygen gradient produced in bulk bars of Bi-2212 during isothermal melt processing can be used to promote the development of uniaxial texture in bulk samples of $Bi_2Sr_2CaCu_2O_y$ (Bi-2212) when combined with a second texturing mechanism such as a set of parallel silver plates. Anisotropy measurements of the critical current in applied magnetic fields showed an increase in performance of approximately two. Comparison with Bi-2212 films showed that significant portions of the textured bars were still misaligned and room for improvement remains with the optimization of this processing approach.

Acknowledgements

This work was performed under the auspices of the United States Department of Energy, Office of Energy Management under contract number W-7405-ENG-36.

References

[1] T. Sasaoka, K. Nomura, J. Sato, S. Kuma, H. Fuijshiro, M. Ikebe, K. Noto, Appl. Phys. Lett. 64 (1994) 1304.
[2] J. Bock, E. Preisler, Solid State Commun. 72 (1989) 453.
[3] N. Chen, A.C. Biondo, S.E. Dorris, K.C. Goretta, M.T. Lanagan, C.A. Youngdahl, R.B. Poeppel, Supercond. Sci. Technol. 6 (1993) 674.
[4] D. Gazit, R.S. Fiegelson, J. Cryst. Growth 91 (1988) 970.
[5] A. Kurosaka, M. Aoyagi, H. Tominaga, O. Fukuda, H. Osanai, Appl. Phys. Lett. 55 (1989) 390.
[6] D.R. Watson, M. Chen, J.E. Evetts, Supercond. Sci. Technol. 8 (1995) 311.
[7] T.G. Holesinger, D.J. Miller, H.K. Viswanathan, K.W. Dennis, L.S. Chumbley, P.W. Winandy, A.C. Youngdahl, Appl. Phys. Lett. 63 (1993) 982.
[8] T.G. Holesinger, D.S. Phillips, J.Y. Coulter, J.O. Willis, D.E. Peterson, Physica C 243 (1995) 93.
[9] T.G. Holesinger, J.M. Johnson, J.Y. Coulter, H. Safar, D.S. Phillips, J.F. Bingert, B.L. Bingham, M.P. Maley, J.L. Smith, D.E. Peterson, Physica C 253 (1995) 182.
[10] T.G. Holesinger, J. Mater. Res. 11 (1996) 2135.
[11] T.G. Holesinger, D.J. Miller, L.S. Chumbley, J. Mater. Res. 7 (1992) 1658.
[12] F. Legendre, L. Schmirgeld-Mignot, P. Regnier, H. Safar, J.Y. Coulter, M. Maley, in: B. Battlogg, C.W. Chu, W.K. Chu, D.U. Gubser, K.A. Müller (Eds.), Proc. 10th Anniversary HTS Workshop on Physics, Materials, and Applications, World Scientific, Singapore, 1997, p. 203.
[13] A. Gurevitch, A.E. Pashitski, H.S. Edelman, D.C. Larbalestier, Appl. Phys. Lett. 62 (1993) 1688.
[14] Q.Y. Hu, H.W. Weber, S.X. Dou, H.K. Liu, H.W. NeumYller, J. Alloys Compounds 195 (1993) 515.
[15] J.O. Willis, J.Y. Coulter, E.J. Peterson, G.F. Chen, L.L. Daemen, L.N. Bulaevskii, M.P. Maley, G.N. Riley, Jr., W.L. Carter, S.E. Dorris, M.T. Lanagan, B.C. Prorok, in: R.P. Reed, F.R. Fickett, L.T. Summers, M. Stieg (Eds.), Advances in Cryogenics Engineering —Materials, vol. 40A, Plenum, New York, 1994, p. 9.
[16] W. Zhang, E.E. Hellstrom, Physica C 218 (1993) 141.